How does gravity save or kill Q-balls?

Takashi Tamaki*

Department of Physics, General Education, College of Engineering, Nihon University, Tokusada, Tamura, Koriyama, Fukushima 963-8642, Japan

Nobuyuki Sakai[†]

Department of Education, Yamagata University, Yamagata 990-8560, Japan (Dated: March 22, 2022)

We explore stability of gravitating Q-balls with potential $V_4(\phi) = \frac{m^2}{2}\phi^2 - \lambda\phi^4 + \frac{\phi^6}{M^2}$ via catastrophe theory, as an extension of our previous work on Q-balls with potential $V_3(\phi) = \frac{m^2}{2}\phi^2 - \mu\phi^3 + \lambda\phi^4$. In flat spacetime Q-balls with V_4 in the thick-wall limit are unstable and there is a minimum charge Q_{\min} , where Q-balls with $Q < Q_{\min}$ are nonexistent. If we take self-gravity into account, on the other hand, there exist stable Q-balls with arbitrarily small charge, no matter how weak gravity is. That is, gravity saves Q-balls with small charge. We also show how stability of Q-balls changes as gravity becomes strong.

PACS numbers: 04.40.-b, 05.45.Yv, 95.35.+d

I. INTRODUCTION

Q-balls [1], a kind of non-topological solitons [2], appear in a large family of field theories with global U(1) (or more) symmetry, and could play important roles in cosmology. For example, the Minimal Supersymmetric Standard Model may contain baryonic Q-balls, which could be responsible for baryon asymmetry [3] and dark matter [4].

Because Q-balls are typically supposed to be microscopic objects, their self-gravity is usually ignored. Therefore, stability of Q-balls has been intensively studied in flat spacetime [5–7]. Q-balls in arbitrary dimension [8] and spinning Q-balls [9, 10] have also been studied.

If Q-balls are so large or so massive, on the other hand, their size becomes astronomical and their gravitational effects are remarkable [10, 11]. For example, it has been shown [12] that the size of Q-balls is bounded above due to gravity. There are analogous objects which are analogous to gravitating Q-balls: boson stars [13]. While Q-balls exist even in flat spacetime, boson stars are supported by gravity and nonexistent in flat spacetime. Although a difference in theory between Q-balls and boson stars is solely the potential parameters, investigations of their properties have been carried out separately so far.

In our previous paper [14], to obtain a unified picture of Q-balls and boson stars, we made an analysis of gravitating Q-balls and boson stars via catastrophe theory [15]. In Ref.[14] we chose a potential for Q-balls

$$V_3(\phi) := \frac{m^2}{2} \phi^2 - \mu \phi^3 + \lambda \phi^4$$
, with m^2 , μ , $\lambda > 0$, (1.1)

because in the limit of $\mu \to 0$ this approaches a typical

potential for boson stars,

$$V_{BS}(\phi) := \frac{m^2}{2}\phi^2 + \lambda\phi^4, \text{ with } m^2, \ \lambda > 0.$$
 (1.2)

As a result, we found that Q-balls and boson stars expose a similar phase relation between a charge and a total Hamiltonian energy. (See, cusp structures in Figs.1(a) and 12(a) in [14].)

In this paper we extend our analysis via catastrophe theory to a potential

$$V_4(\phi) := \frac{m^2}{2} \phi^2 - \lambda \phi^4 + \frac{\phi^6}{M^2} \text{ with } m^2, \lambda, M > 0, (1.3)$$

which we call V_4 Model [16]. We choose this potential because previous work on Q-balls in flat spacetime [6, 7] showed stability of Q-balls with V_3 Model (1.1) and V_4 Model (1.3) are quite different. We are interested in how gravitating Q-balls properties depend on potentials and what universal properties are.

This paper is organized as follows. In Sec. II, we derive equilibrium field equations. In Sec. III, we show numerical results of equilibrium Q-balls and discuss their stability. In Sec. IV, we discuss why thick-wall solutions become stable against the naive expectation that gravity is not effective for Q-balls with small charge. In Sec. V, we devote to concluding remarks.

II. ANALYSIS METHOD OF EQUILIBRIUM Q-BALLS

A. Equilibrium field equations

We begin with the action

$$S = \int d^4x \sqrt{-g} \left\{ \frac{\mathcal{R}}{16\pi G} - \frac{1}{2} g^{\mu\nu} \partial_{\mu} \phi \cdot \partial_{\nu} \phi - V(\phi) \right\}, \tag{2.1}$$

^{*}Electronic address: tamaki@ge.ce.nihon-u.ac.jp

 $^{^\}dagger Electronic address:$ nsakai@e.yamagata-u.ac.jp

where $\phi = (\phi_1, \phi_2)$ is an SO(2)-symmetric scalar field and $\phi := \sqrt{\phi \cdot \phi} = \sqrt{\phi_1^2 + \phi_2^2}$. We assume a spherically symmetric and static spacetime,

$$ds^{2} = -\alpha^{2}(r)dt^{2} + A^{2}(r)dr^{2} + r^{2}(d\theta^{2} + \sin^{2}\theta d\varphi^{2}). \tag{2.2}$$

For the scalar field, we assume that it has a spherically symmetric and stationary form,

$$(\phi_1, \phi_2) = \phi(r)(\cos \omega t, \sin \omega t). \tag{2.3}$$

Then the field equations become

$$-\frac{rA^3}{2}G_t^t := A' + \frac{A}{2r}(A^2 - 1)$$

$$= 4\pi G r A^3 \left(\frac{{\phi'}^2}{2A^2} + \frac{\omega^2 \phi^2}{2\alpha^2} + V\right), \quad (2.4)$$

$$\frac{r\alpha}{2}G_{rr} := \alpha' + \frac{\alpha}{2r}(1 - A^2)$$

$$= 4\pi G r \alpha A^2 \left(\frac{{\phi'}^2}{2A^2} + \frac{\omega^2 \phi^2}{2\alpha^2} - V\right), \quad (2.5)$$

$$\frac{A^2 \phi}{\phi_1} \Box \phi_1 := \phi'' + \left(\frac{2}{r} + \frac{\alpha'}{\alpha} - \frac{A'}{A}\right) \phi' + \left(\frac{\omega A}{\alpha}\right)^2 \phi$$

$$= A^2 \frac{dV}{d\phi}, \quad (2.6)$$

where ' := d/dr. To obtain Q-ball solutions in curved spacetime, we should solve (2.4)-(2.6) with boundary conditions,

$$A(0) = A(\infty) = \alpha(\infty) = 1,$$

 $A'(0) = \alpha'(0) = \phi'(0) = \phi(\infty) = 0.$ (2.7)

We also restrict our solutions to monotonically decreasing $\phi(r)$. Due to the symmetry, there is a conserved charge called Q-ball charge,

$$Q := \int d^3x \sqrt{-g} g^{0\nu} (\phi_1 \partial_\nu \phi_2 - \phi_2 \partial_\nu \phi_1) = \omega I,$$
where
$$I := 4\pi \int \frac{Ar^2 \phi^2}{\alpha} dr.$$
 (2.8)

We suppose V_4 Model (1.3). Rescaling the quantities

$$\begin{split} \tilde{t} &:= \lambda M t, \quad \tilde{r} := \lambda M r, \quad \tilde{\phi} := \frac{\phi}{\sqrt{\lambda} M}, \\ \tilde{V}_4 &:= \frac{V_4}{\lambda^3 M^4} = \frac{\tilde{m}^2}{2} \tilde{\phi}^2 - \tilde{\phi}^4 + \tilde{\phi}^6, \\ \tilde{m} &:= \frac{m}{\lambda M}, \quad \tilde{\omega} := \frac{\omega}{\lambda M}, \quad \kappa := G \lambda M^2, \end{split}$$
 (2.9)

the field equations (2.4)-(2.6) with the potential (1.3) are rewritten as

$$A' + \frac{A}{2\tilde{r}}(A^2 - 1) = 4\pi\kappa\tilde{r}A^3 \left(\frac{\tilde{\phi}'^2}{2A^2} + \frac{\tilde{\omega}^2\tilde{\phi}^2}{2\alpha^2} + \tilde{V}_4\right),$$
(2.10)

$$\alpha' + \frac{\alpha}{2\tilde{r}}(1 - A^2) = 4\pi\kappa\tilde{r}\alpha A^2 \left(\frac{\tilde{\phi}'^2}{2A^2} + \frac{\tilde{\omega}^2\tilde{\phi}^2}{2\alpha^2} - \tilde{V}_4\right),\tag{2.11}$$

$$\tilde{\phi}'' + \left(\frac{2}{\tilde{r}} + \frac{\alpha'}{\alpha} - \frac{A'}{A}\right)\tilde{\phi}' + \left(\frac{\tilde{\omega}A}{\alpha}\right)^2\tilde{\phi} = A^2 \frac{d\tilde{V}_4}{d\tilde{\phi}}. \quad (2.12)$$

B. Stability analysis method via catastrophe theory

In our previous paper [14], we discussed how we apply catastrophe theory to the Q-ball and boson star systems. Here, we summarize our method. An essential point is to choose behavior variable(s), $control\ parameter(s)$ and a potential in the Q-ball system appropriately.

We use the Hamiltonian energy E as a potential because $\delta E/\delta \phi|_Q = \delta E/\delta g_{\mu\nu} = 0$, reproduces the equilibrium field equations (2.4)-(2.6). The Hamiltonian energy E was calculated as [14]

$$E = \lim_{r \to \infty} \frac{r^2 \alpha'}{2GA} = \frac{M_S}{2},\tag{2.13}$$

where M_S is the Schwarzschild mass. We also normalize E and Q as

$$\tilde{E} := \frac{E}{M}, \quad \tilde{Q} := Q\lambda.$$
 (2.14)

Because the charge \tilde{Q} and the model parameters \tilde{m}^2 and κ specify the system environment, they should be regarded as control parameters. To discuss a behavior variable we consider a one-parameter family of perturbed field configurations $\phi_x(r)$ near the equilibrium solution $\phi(r)$. Because $dE[\phi_x]/dx = (\delta E/\delta \phi_x)d\phi_x/dx = 0$ when ϕ_x is an equilibrium solution, x is a behavior variable.

According to Thom's theorem, if the system has two control parameters, there is essentially one behavior variable; if the system has three control parameters, there are one or two behavior variables. Because the present Q-ball system contains $(\tilde{Q}, \tilde{m}^2, \kappa)$, we speculate that each has two behavior variables, $\tilde{\omega}^2$ and $\tilde{\phi}(0)$. However, because stability structure of equilibrium solutions in three-parameter space $(\tilde{Q}, \tilde{m}^2, \kappa)$ is very complicated and our interest is how gravitational effects change the stability structure, in what follows, we discuss the stability structure of equilibrium solutions in two-parameter space (\tilde{Q}, κ) under fixed \tilde{m}^2 .

Our method of analyzing the stability of Q-balls is as follows.

- Fix the value of \tilde{m}^2 .
- Solve the field equations (2.4)-(2.6) with the boundary condition (2.7) numerically to obtain equilibrium solutions $\tilde{\phi}(r)$ for various values of $\tilde{\omega}$ and κ .
- Calculate \tilde{Q} for each solution to obtain the equilibrium space $\mathcal{M} = \{(x, \tilde{Q}, \kappa)\}$. We denote the equation that determines \mathcal{M} by $f(x, \tilde{Q}, \kappa) = 0$.

- Find folding points where $\partial \tilde{Q}/\partial x = 0$ or $\partial \kappa/\partial x = 0$, in \mathcal{M} , which are identical to the stability-change points, $\Sigma = \{(x, \tilde{Q}, \kappa) | \partial f/\partial x = 0, f = 0\}.$
- Calculate the energy \tilde{E} by (2.13) for equilibrium solutions around a certain point in Σ to find whether the point is a local maximum or a local minimum. Then we find the stability structure for the whole \mathcal{M} .

III. EQUILIBRIUM SOLUTIONS AND THEIR STABILITY

In preparation for discussing gravitating Q-balls, we review their equilibrium solutions and stability in flat spacetime ($\kappa = 0$). The scalar field equation (2.12) reduces to

$$\tilde{\phi}'' = -\frac{2}{\tilde{r}}\tilde{\phi}' - \tilde{\omega}^2\tilde{\phi} + \frac{d\tilde{V}_4}{d\tilde{\phi}}.$$
 (3.1)

This is equivalent to the field equation for a single static scalar field with the potential $V_{\omega} := \tilde{V}_4 - \tilde{\omega}^2 \tilde{\phi}^2/2$. Equilibrium solutions satisfying boundary conditions (2.7) exist if $\min(V_{\omega}) < \tilde{V}_4(0)$ and $d^2V_{\omega}/d\tilde{\phi}^2(0) > 0$, which is equivalent to

$$0 < \epsilon^2 < \frac{1}{2},\tag{3.2}$$

where $\epsilon := \sqrt{\tilde{m}^2 - \tilde{\omega}^2}$. The two limits $\epsilon^2 \to \frac{1}{2}$ and $\epsilon \to 0$ correspond to the thin-wall limit and the thick-wall limit, respectively.

It is usually assumed that the potential has an absolute minimum at $\phi=0$. If V(0) is a local minimum but the absolute minimum is located at $\phi\neq 0$, true vacuum bubbles with charge (Q-bubbles) may appear. The condition for Q-bubbles is $\tilde{m}^2<0.5$. Therefore, stability structure falls into two classes, $\tilde{m}^2<0.5$ and $\tilde{m}^2\geq0.5$ [7]:

- $\tilde{m}^2 \geq 0.5$: For each \tilde{m}^2 , there is a nonzero minimum charge, \tilde{Q}_{\min} , below which equilibrium solutions do not exist. For $\tilde{Q} > \tilde{Q}_{\min}$, stable and unstable solutions coexist.
- $\tilde{m}^2 < 0.5$: For each \tilde{m}^2 , there is a maximum charge, \tilde{Q}_{\max} , as well as a minimum charge, \tilde{Q}_{\min} , where one stable and two unstable solutions coexist for $\tilde{Q}_{\min} < \tilde{Q} < \tilde{Q}_{\max}$. For $\tilde{Q} < \tilde{Q}_{\min}$ or $\tilde{Q} > \tilde{Q}_{\max}$, there is one unstable solution.

To discuss gravitational effects later, it is useful to estimate the central value $\tilde{\phi}(0)$ in flat spacetime. Because $V_{\omega}=0$ at spacial infinity, its order of magnitude is estimated as a solution of $V_{\omega}=0$ ($\tilde{\phi}(0)\neq 0$). For V_4 with the thick-wall condition $\epsilon\ll 1$, we obtain

$$\tilde{\phi}^2(0) \simeq \frac{1 - \sqrt{1 - 2\epsilon^2}}{2} \simeq \frac{\epsilon^2}{2}.$$
 (3.3)

Thus, $\tilde{\phi}(0) \sim \epsilon$.

It was shown [14] that in V_3 Model properties of gravitating Q-balls also depend on whether $\tilde{m}^2 \geq 0.5$ or $\tilde{m}^2 < 0.5$. In the following analysis, therefore, we choose $\tilde{m}^2 = 0.6$ and 0.3 typically. Other cases are not qualitatively different from these cases. For our numerical calculation, we use the Bulirsch-Stoer method based on the double precision FORTRAN program.

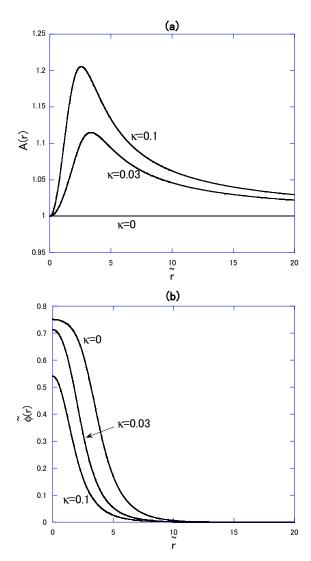


FIG. 1: Behavior of the metric A(r) and $\tilde{\phi}(r)$ for the solutions $\tilde{\omega}^2 \simeq 0.34$ in (a) and (b), respectively. We find that the scalar field is concentrated near the origin as shown in (b). This tendency becomes stronger as gravity is stronger. Thus, A(r) varies near the origin compared with that in the thick-wall solutions.

A. Gravitating Q-balls for $\tilde{m}^2 \geq 0.5$

In this subsection we fix $\tilde{m}^2 = 0.6$. First, we present typical solutions in Figs. 1 and 2: we choose $\kappa = 0$,

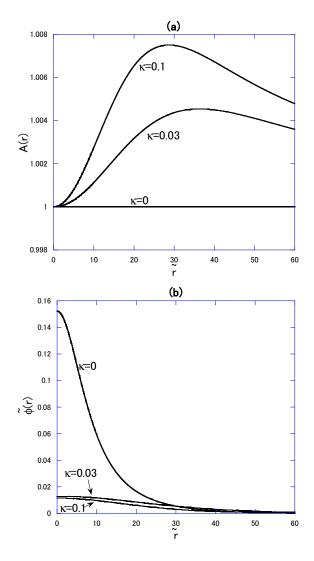


FIG. 2: Behavior of the metric $A(r) := \sqrt{g_{rr}}$ and $\tilde{\phi}(r)$ for the thick-wall solutions $\tilde{\omega}^2 \simeq 0.595$ in (a) and (b), respectively.

0.03, and 0.1 and show the metric A(r) in (a) and the scalar field amplitude $\tilde{\phi}(r)$ in (b). In Figs. 1 we put $\tilde{\omega}^2 \simeq 0.34$. We find that as κ becomes larger, or gravity is stronger, $|A(r)^2-1|$ becomes up to order one, and the Q-ball size becomes smaller by self-gravity. As we shall discuss below, the solutions with $\kappa=0,0.03$ in Figs. 1 are stable, while the solution with $\kappa=0.1$ is unstable. That is, strong gravity destabilizes or kills some of the solutions which would be existent and stable without gravity.

Figs. 2 show the solutions with $\tilde{\omega}^2 \simeq 0.595$. Because $\epsilon^2 = 0.05 \ll 1$, these are thick-wall solutions. We find an interesting feature in (b): the difference between $\tilde{\phi}$ with $\kappa = 0.03$ and $\kappa = 0.1$ are small, but they are quite different from $\tilde{\phi}(r)$ with $\kappa = 0$. This indicates that the configuration of $\tilde{\phi}(r)$ for gravitating Q-balls does not approach that for $\kappa = 0$ if we take the limit of $\kappa \to 0$. In the next section we shall discuss the reason for this.

In this way we calculate equilibrium solutions numer-

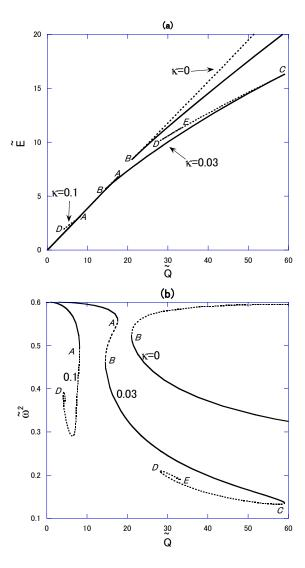


FIG. 3: (a) \tilde{Q} - \tilde{E} and (b) \tilde{Q} - $\tilde{\omega}^2$ relations for $\tilde{m}^2=0.6$ with $\kappa=0,\,0.03$ and 0.1. For the flat case $\kappa=0$, it has been found that solutions with solid (dotted) lines are stable (unstable) [7]. We extend these interpretations for the gravitating case.

ically for various $\tilde{\omega}^2$ and show \tilde{Q} - \tilde{E} and \tilde{Q} - $\tilde{\omega}^2$ relations in Figs. 3. We can obtain stability of the solutions using catastrophe theory as follows.

- When there are multiple values of \tilde{E} for a given set of the control parameters $(\tilde{m}^2, \kappa, \tilde{Q})$, by energetics the solution with the lower value of \tilde{E} should be stable.
- Once the stability for a given set of the parameters $(\tilde{m}^2, \kappa, \tilde{Q})$ is found, the stability for all sets of parameters which are reached continuously from that set without crossing turning points (i.e., stability-change points Σ) is the same.
- Stability changes across Σ .
- Spiral structure in the \tilde{Q} - $\tilde{\omega}^2$ plane should be consid-

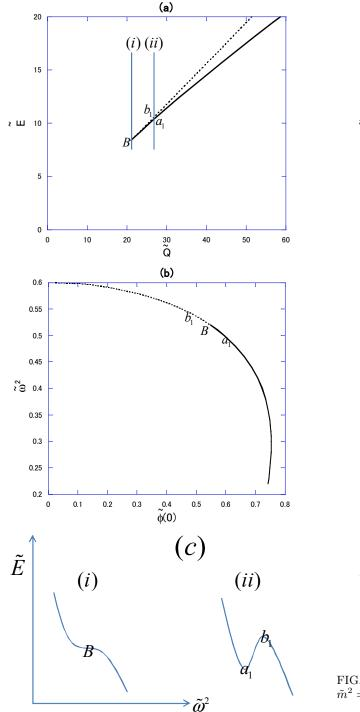


FIG. 4: Stability interpretation via catastrophe theory for $\tilde{m}^2=0.6$ for the flat case.

ered exceptionally. We interpret that all solutions are unstable there.

As a result, we can conclude that solid and dashed lines correspond to stable and unstable solutions, respectively.

To illustrate this energetic or catastrophic argument more clearly, we give a sketch of the potential function \tilde{E}

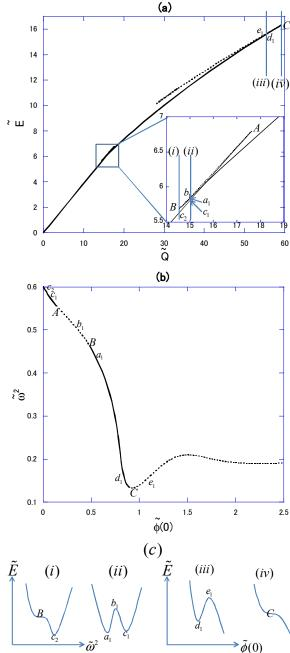


FIG. 5: Stability interpretation via catastrophe theory for $\tilde{m}^2=0.6$ for $\kappa=0.03$.

near the equilibrium solutions in Figs. 4 and 5. Figs. 4 shows the flat case ($\kappa = 0$): the solid (dotted) line in (a) and the points B, a_1 and b_1 correspond to those in (b), where candidates of behavior variables $\tilde{\phi}(0)$ and $\tilde{\omega}^2$ are shown. (c) is a schematic picture of the potential function \tilde{E} in terms of the behavior variable $\tilde{\omega}^2$. The point B, the cusp in (a), corresponds to the inflection point in (c); we understand why there is no solution with lower \tilde{Q} . The point a_1 on the solid line and the point b_1 on the dotted line in (ii) correspond to the potential minimum and the

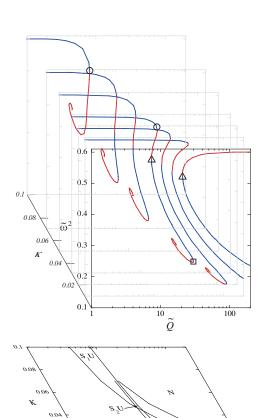


FIG. 6: Structures of the equilibrium spaces, $M = \{(\tilde{\omega}^2, \kappa, \tilde{Q})\}$, and their catastrophe map, $\chi(M)$, into the control planes, $C = \{(\kappa, \tilde{Q})\}$, for $\tilde{m}^2 = 0.6$. Blue lines and red lines in M represent stable and unstable solutions, respectively. In the regions denoted by S_1 , S_iU (i = 1, 2) and N on C, there are one stable solution, i stable solution(s) and one or more unstable solution(s), and no equilibrium solution, respectively, for fixed (κ, \tilde{Q}) .

 U, \mathcal{E}

maximum in (c), respectively.

As another example for catastrophic interpretation, we discuss stability of the solutions for $\kappa=0.03$, using Figs. 5. A complicated structure appears in the enlargement in (a). In the Q-range between A and B there are triple values of \tilde{E} for fixed Q. In this case the potential function should be given by (ii) in (c). This means that two stable solutions coexist for fixed Q in this range. As a result, we can conclude that there are stable gravitating Q-balls which approach $\tilde{Q} \to 0$ in the thick-wall limit ($\tilde{\omega}^2 \to 0.6$). Fig. 5 (b) tells us that in the unstable sequence right the point C there is no one-to-one correspondence between $\tilde{\omega}^2$ and the solutions while there is one-to-one correspondence between $\tilde{\phi}(0)$ and the solutions. In this range, therefore, $\tilde{\phi}(0)$ is more appropriate

as a behavior variable than $\tilde{\omega}^2$ as shown in (iii) and (iv) in (c).

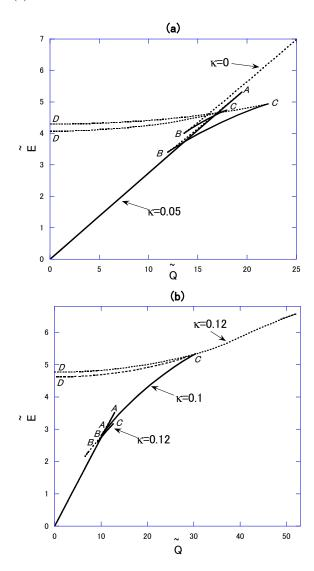


FIG. 7: \tilde{Q} - \tilde{E} relations for $\tilde{m}^2=0.3$ with $\kappa=0$ and 0.05 in (a) and with $\kappa=0.1$ and 0.12 in (b), respectively. As in the case for $\tilde{m}^2=0.6$, gravitating cases have sequences from A to the origin, which are considered to be stable, written by solid lines. For $\kappa=0.12$, the sequence from B-C-D separates into two parts. Each branch has sequences of cusp structures (around $\tilde{Q}\sim 8$ and 48 in (b)).

Fig. 6 shows the structures of the equilibrium spaces, $\mathcal{M} = \{(\tilde{\omega}^2, \kappa, \tilde{Q})\}$, and their catastrophe map, $\chi(\mathcal{M})$, into the control planes, $C = \{(\kappa, \tilde{Q})\}$, for $\tilde{m}^2 = 0.6$. In the regions denoted by S_1 , S_iU (i=1,2) and N on C, there are one stable solution, i stable solution(s) and one or more unstable solution(s), and no equilibrium solution, respectively, for fixed (κ, \tilde{Q}) . The points A, B and C in Figs. 3 are marked by circles, triangles and squares, respectively. For example, for $\kappa = 0.1$, which is the case shown in Figs. 3, we can confirm that only a stable solution exists below $\tilde{Q} \sim 4$ (the point D) which is denoted

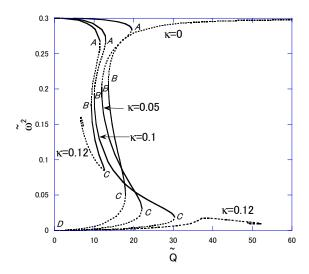


FIG. 8: \tilde{Q} - $\tilde{\omega}^2$ relation for the same solutions as in Figs. 7. The points from A to D and the dotted (solid) lines correspond to those in Figs. 7. From this correspondence, we find that flat Q-balls approach $\tilde{Q} \to \infty$ in the thick-wall limit $\tilde{\omega}^2 \to 0.3$ while gravitating Q-balls approach $\tilde{Q} \to 0$ in this limit as in the case for $\tilde{m}^2 = 0.6$.

by S_1 in Fig. 6. One stable solution and one or more unstable solution(s) exist in the region from $\tilde{Q} \sim 4$ to $\tilde{Q} \sim 8$ (the point A) which is denoted by S_1U .

Main characteristics of the equilibrium solutions in Figs. 3 and 6 are summarized as follows.

- If $\kappa = 0$, there is a minimum charge, Q_{\min} , denoted by B on the $\kappa = 0$ line in Fig. 3. The equilibrium solutions in the thick-wall limit $\epsilon^2 \to 0$ are unstable, as indicated by the dotted lines.
- If $\kappa \neq 0$, no matter how small κ is, the equilibrium solutions in the thick-wall limit $\epsilon^2 \to 0$ are stable and $\tilde{Q} \to 0$. These stable solutions correspond to the solid lines from $\tilde{Q} = 0$ to A in Fig. 3. We can interpret that gravity saves thick-wall Q-balls.
- If $\kappa \neq 0$, the maximum charge, Q_{max} , emerges in the thin-wall range. This extreme solution is denoted by C on the $\kappa = 0.03$ line in Fig. 3. That is, gravity kills Q-balls with large charge.
- If $\kappa \neq 0$, spiral trajectories appear in the \tilde{Q} - $\tilde{\omega}^2$ plane.
- If $\kappa \simeq 0.1$, the two extremal solutions B and C merge and disappear, and accordingly the stability sequence between them disappear, too.

The second result is remarkable. In Sec. IV, we investigate why these discontinuous changes occur at $\kappa = 0$.

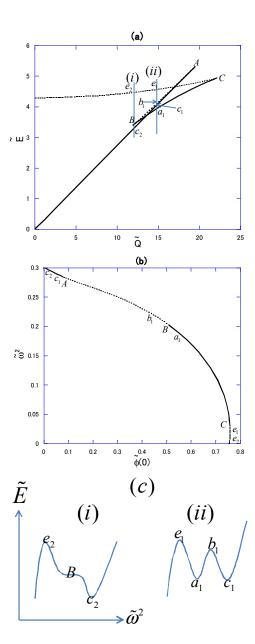


FIG. 9: Stability interpretation via catastrophe theory for $\tilde{m}^2=0.3$ and $\kappa=0.05.$

B. Gravitating Q-balls for $\tilde{m}^2 < 0.5$

In this subsection we fix $\tilde{m}^2 = 0.3$. We show \tilde{Q} - \tilde{E} relations in Figs. 7 and \tilde{Q} - $\tilde{\omega}^2$ relations in Fig. 8. In the same method as in Sec. III A, we can determine stability of the equilibrium solutions: solid lines and dashed lines correspond to stable and unstable solutions, respectively.

In the case of $\kappa=0$, for example, there are two cusp structures as shown in Figs. 7 (a). Only solutions in the narrow range between B and C are stable. As another example, for $\kappa=0.05$ we illustrate catastrophic interpretation in Figs. 9. In the Q-range between A and B there are quadruple values of \tilde{E} for fixed \tilde{Q} . In this case the potential function is given by (ii) in (c). As in the

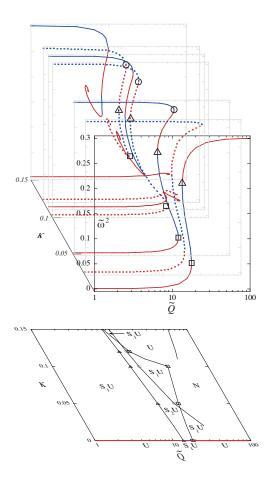


FIG. 10: Structures of the equilibrium spaces, $M = \{(\tilde{\omega}^2, \kappa, \tilde{Q})\}$, and their catastrophe map, $\chi(M)$, into the control planes, $C = \{(\kappa, \tilde{Q})\}$, for $\tilde{m}^2 = 0.3$. Blue lines and red lines in M represent stable and unstable solutions, respectively. In the regions denoted by S_iU (i = 1, 2) and N on C, there are i stable solution(s) and one or more unstable solution(s), and no equilibrium solution, respectively, for fixed (κ, \tilde{Q}) .

case of $\tilde{m}^2 = 0.6$ and $\kappa = 0.03$ in Fig. 5, two stable solutions coexist for fixed Q in this range, and there are stable gravitating Q-balls which approach $\tilde{Q} \to 0$ in the thick-wall limit ($\tilde{\omega}^2 \to 0.3$).

Figure 10 shows the structures of the equilibrium spaces, $\mathcal{M} = \{(\tilde{\omega}^2, \kappa, \tilde{Q})\}$, and their catastrophe map, $\chi(\mathcal{M})$, into the control planes, $C = \{(\kappa, \tilde{Q})\}$, for $\tilde{m}^2 = 0.3$. $\chi(\mathcal{M})$ shows that in the regions denoted by S_iU (i=1,2) and N on C, there are i stable solution(s) and one or more unstable solution(s), and no equilibrium solution, respectively, for fixed (κ, \tilde{Q}) . The points A, B and C in Figs. 7 are marked by circles, triangles and squares, respectively. For example, for $\kappa = 0.05$, if we fix \tilde{Q} between $\simeq 12$ (the point B) and $\simeq 18$ (the point A), there are two stable solutions and one (or more) unstable

solution(s).

Main characteristics of the equilibrium solutions in Figs. 7, 8 and 10 are summarized as follows.

- If κ = 0, there is a maximum charge for stable solutions, Q_{max}, denoted by C, as well as a minimum charge, Q_{min}, denoted by B, on the κ = 0 line in Figs. 7, 8. The equilibrium solutions in the thickwall limit ϵ² → 0 are unstable, as indicated by the dotted lines.
- If $\kappa \neq 0$, no matter how small κ is, the equilibrium solutions in the thick-wall limit $\epsilon^2 \to 0$ are stable and $\tilde{Q} \to 0$. These stable solutions correspond to the solid lines from $\tilde{Q} = 0$ to A in Figs. 7. We can interpret that gravity saves thick-wall Q-balls.
- As κ increases, the maximum charge, $Q_{\rm max}$, increases until $\kappa = \kappa_{\rm crit} \simeq 0.1$.
- The solution sequence for fixed κ splits into two when $\kappa = \kappa_{\rm crit}$. In each sequence spiral trajectories appear in the \tilde{Q} - $\tilde{\omega}^2$ plane.

IV. THICK-WALL LIMIT

It is not surprising that properties of gravitating Q-balls change gradually as κ increases. It seems strange, however, properties of gravitating Q-balls in the limit of $\kappa \to 0$ differs completely from that of flat Q-balls ($\kappa = 0$), as show in Figs. 6 and 10. Here we discuss the reason for this.

We consider the case of weak gravity ($\kappa \ll 1$) and thick-wall ($\epsilon^2 \ll 1$). Since the gravity is weak, we can express the metric functions as

$$\alpha^2 = 1 + h(r), \quad A^2 = 1 + f(r), \quad (h \ll 1, \quad f \ll 1). \quad (4.1)$$

Up to first order in h and f, we can rewrite the scalar field equation (2.6) as

$$\tilde{\phi}'' + \left(\frac{2}{\tilde{r}} + \frac{h'}{2} - \frac{f'}{2}\right)\tilde{\phi}' = (1+f)[(\epsilon^2 + h\tilde{\omega}^2)\tilde{\phi}^2 - 4\tilde{\phi}^3 + 6\tilde{\phi}^5].$$
(4.2)

If we fix $\epsilon^2 > 0$ and take the limit of $\kappa \to 0$ (i.e., $h, f \to 0$), Eq.(4.2) reduces to the field equation in flat spacetime, (3.1). However, if we take the limit of $\epsilon^2 \to 0$ as well, the situation becomes complicated. For any small κ , if we take so small ϵ^2 that $\epsilon^2 \ll h\tilde{\omega}^2$, which means $\epsilon^2 \ll \kappa \tilde{\omega}^4$ as we shall show below, the first order term in $h, h\tilde{\omega}^2\tilde{\phi}^2$, dominates the zeroth order term, $\epsilon^2\tilde{\phi}^2$. That is, in the thick-wall limit of $\epsilon^2 \to 0$, the scalar field equation with infinitesimally small κ can be different from that with $\kappa = 0$.

The above argument is based on the hypothesis that h does not approach zero as fast as ϵ^2 when we take the limit of $\epsilon \to 0$. Otherwise, the inequality $\epsilon^2 < h\tilde{\omega}^2$ would

be wrong. To complete this argument, we shall estimate the order of magnitude of h by assuming

$$\tilde{\phi}(\tilde{r}) \sim \epsilon \ll 1 \text{ for } \tilde{r} < \frac{1}{\epsilon},$$
 (4.3)

which is valid in flat spacetime. From the Einstein equations, we find

$$-G_t^t + G_i^i := \left(\frac{\tilde{r}^2 \alpha'}{A}\right)' = 8\pi \kappa \tilde{r}^2 A \alpha \left(\frac{\tilde{\omega}^2 \tilde{\phi}^2}{\alpha^2} - V\right), \tag{4.4}$$

where i runs spacial components. If we take the weak field approximation (4.1) and the thick-wall approximation $\epsilon^2 \ll 1$, we obtain

$$(\tilde{r}^2 h')' \simeq 8\pi \kappa \tilde{r}^2 \tilde{m}^2 \tilde{\phi}^2 . \tag{4.5}$$

With the boundary condition h'(0) = 0 and the approximation (4.3), we can integrate (4.5) as

$$h' \simeq \frac{8}{3}\pi\kappa \tilde{m}^2 \epsilon^2 \tilde{r}, \text{ for } \tilde{r} < \frac{1}{\epsilon}.$$
 (4.6)

With the boundary condition $h(\infty) = 0$ and the approximation (4.3), we can integrate (4.6) as

$$h \simeq \frac{4}{3}\pi\kappa \tilde{m}^2 (\epsilon^2 \tilde{r}^2 - 1), \text{ for } \tilde{r} < \frac{1}{\epsilon}.$$
 (4.7)

This means $h \sim \kappa \tilde{m}^2$, which is independent of ϵ . Therefore, we can conclude $\epsilon^2 \ll h \tilde{\omega}^2$ in (4.2) in the thick-wall limit with fixed κ .

If the assumption (4.3) is not valid, the configuration of $\tilde{\phi}(\tilde{r})$ is quite different from that for flat spacetime. This case also means that gravitating Q-balls are completely different from those in flat case even if the gravity is very weak.

From the above argument, we can understand why gravity saves thick-wall Q-balls. This is not surprising because similar phenomenon occurs in the case of boson stars: boson stars with $V_{\rm BS}$ do not exist in flat case while they exist even if the gravity is very weak.

V. CONCLUSION AND DISCUSSION

We have analyzed stability of gravitating Q-balls with V_4 via catastrophe theory. Our results are summarized

as follows.

Although our original concern was massive Q-balls with astronomical size, we have found an unexpected result that the weak gravity changes properties of thickwall Q-balls. In flat spacetime Q-balls in the thick-wall limit are unstable and there is a minimum charge Q_{\min} , where Q-balls with $Q < Q_{\min}$ are nonexistent. If we take self-gravity into account, on the other hand, there exist stable Q-balls with arbitrarily small charge, no matter how weak gravity is. That is, gravity saves Q-balls with small charge.

This result indicates that gravitational effects may be important for other models, such as Q-balls in supersymmetric extensions of the Standard Model. For example, gravity may allow for a new branch of solutions in some parameter range where equilibrium solutions are nonexistent in the absence of gravity.

We have also shown how stability of Q-balls changes as gravity becomes strong. For example, if $m^2 \geq 0$, the maximum charge, $Q_{\rm max}$, decreases as gravity becomes strong, while there is no maximum charge in flat spacetime. That is, gravity kills thin-wall Q-balls with large charge.

In the case of strong gravity, only Q-balls with small charge exist, and instability solutions make spiral trajectories in the \tilde{Q} - $\tilde{\omega}^2$ plane. These properties are common to Q-balls with V_3 potential and boson stars with $V_{\rm BS}$. While Q-balls and boson stars have been studied separately so far, our result suggest that there is universal nature of gravity, which may be important to discuss Q-balls with astronomical size or boson stars.

Acknowledgments

We would like to thank Kei-ichi Maeda for useful discussion and for continuous encouragement. The numerical calculations were carried out on SX8 at YITP in Kyoto University. This work was supported by MEXT Grant-in-Aid for Scientific Research on Innovative Areas No. 22111502.

^[1] S. Coleman, Nucl. Phys. **B262**, 263 (1985).

^[2] For a review of non-topological solitons in flat spacetime, see, T. Lee and Y. Pang, Phys. Rep. **221**, 251 (1985).

 ^[3] A. Kusenko, Phys.Lett. B 405, 108 (1997) 108; Nucl. Phys. B (Proc. Suppl.) 62A-C, 248 (1998). K. Enqvist and J. McDonald, Phys. Lett. B 425, 309 (1998); Nucl. Phys. B 538, 3210 (1999); S. Kasuya and M. Kawasaki,

Phys. Rev. D 62, 023512 (2000).

^[4] A. Kusenko and M. Shaposhnikov, Phys. Lett. B 418, 46 (1998); K. Enqvist and A. Mazumdar, Phys. Rep. 380, 99 (2003); I. M. Shoemaker and A. Kusenko, Phys. Rev. D 80, 075021 (2009).

 ^[5] A. Kusenko, Phys. Lett. B 404, 285 (1997); 406, 26 (1997); F. V. Kusmartsev, Phys. Rep. 183, 1 (1989). T.

- Multamaki and I. Vilja, Nucl. Phys. B **574**, 130 (2000); M. Axenides, S. Komineas, L. Perivolaropoulos and M. Floratos, Phys. Rev. D **61**, 085006 (2000).
- [6] F. Paccetti Correia and M. G. Schmidt, Eur. Phys. J. C21, 181 (2001).
- [7] N. Sakai and M. Sasaki, Progress of Theoretical Physics, 119, 929 (2008).
- [8] M. Gleiser and J. Thorarinson, Phys. Rev. D 73, 065008 (2006); M. I. Tsumagari, E. J. Copeland, and P. M. Saffin, Phys. Rev. D 78, 065021 (2008).
- [9] M. S. Volkov and E. Wöhnert, Phys. Rev. D 66, 085003 (2002).
- [10] B. Kleihaus, J. Kunz, and M. List, Phys. Rev. D 72, 064002 (2005); B. Kleihaus, J. Kunz, M. List, and I. Schaffer, *ibid.* 77, 064025 (2008).
- [11] R. Friedberg, T. D. Lee, and Y. Pang, Phys. Rev. D 35,

- 3658 (1987). B. W. Lynn, Nucl. Phys. **B321**, 465 (1989); S. B. Selipsky, *ibid.* **B321**, 430,1989; S. Bahcall, *ibid.* **B325**, 606 (1989); A. Prikas, Phys. Rev. D **66**, 025023 (2002); Y. Verbin, *ibid.* **76**, 085018 (2007).
- [12] T. Multamaki and I. Vilja, Phys. Lett. B **542**, 137 (2002).
- [13] For a review of boson stars, see, P. Jetzer, Phys. Rep. 220, 163 (1992). F. E. Schunck and E. W. Mielke, Class. Quantum Grav. 20, R301 (2003).
- [14] T. Tamaki and N. Sakai, Phys. Rev. D 81, 124041 (2010).
- [15] For a review of catastrophe theory, see, e.g., T. Poston and I.N. Stewart, Catastrophe Theory and Its Application, Pitman (1978).
- [16] This model has also been considered in [10]. They fixed the parameter $\tilde{m}^2 > 0.5$ and focused on the rotating case.